CATO Workpackage WP 4.1

Subsurface mineralisation:

Halite precipitation during CO_2 injection

Nadja Müller

Shell Exploratory Research (EPT-RXX)

Submitted 07-12-2007

STUDY OF SALT PRECIPITATION - MODELING TOUGH2

Rijswijk, November 2007
Nadja Müller, Shell EPT-RXX

This deliverable replaces the 3 outstanding deliverables from period May - October 2006, November 2006 - April 2007 and May – October 2007. Instead of 3 deliverables on TOUGHreact and mineralization modeling, the scope has shifted towards a more urgent issue of halite precipitation during CO_2 injection. The problem was modeled with TOUGH2 and new module for CO2-water-NaCl systems, called ECO2N. The results are presented in this report.

I. INTRODUCTION

The injection of dry supercritical CO_2 into brine aquifers has the potential to dry formation waters, due to evaporation effects[1]. Dry supercritical carbon dioxide has the ability to "evaporate" (or dissolve) small amounts of water. This could significantly impair injection rates, as has been noted in gas-storage reservoirs[2]. This work investigates the impact of this "evaporation" phenomenon in porous media, which can lead to severe increases in salinity and salt precipitation. This is of special interest in connection with CO_2 storage in saline aquifers. Carbon storage in the subsurface is among the most promising immediately applicable climate change mitigation measures. CO_2 can be injected as supercritical fluid into deep rock formations and be stored over centuries like natural gas and oil to reduce atmospheric carbon emissions.

The behavior of the flow system is as follows. As dry CO_2 is being injected the formation water is "evaporated". Deep formation water can have solids in solution, which are usually dissolved salts. As the water is removed into the flowing CO_2 stream, salt concentration increases and eventually reaches the solubility limit, giving rise to precipitation of halite. The precipitated solids reduce the pore space available to the fluids and can block the pore throats in the sedimentary rock. The blocked pore throats do not permit fluid movement and hinder any further injection of carbon dioxide. The phenomenon occurs in and close to the borehole, where the dry CO_2 enters the rock formation. Salt precipitation can lead to a positive skin effect and dramatically reduce injectivity. The physical processes involved are complex and include counter flow of aqueous and CO_2-rich phases due to capillary effects, molecular diffusion of dissolved solids in the aqueous phase, and effects from increased density and viscosity of the aqueous phase at the evaporation front.

These phenomena were modeled with a reservoir simulator, TOUGH2[3], and the 1D results are presented in this report.

II. GENERAL:

1. Properties of the CO_2 injection reservoir

The initial p-T conditions of the reservoir are 35°C and 65 bar, containing a 200 ppk NaCl brine. Carbon dioxide is injected at 55°C and 73 bar at bottom hole conditions. In total, 60.000 tons of carbon dioxide are sequestered in the reservoir over a time period of 2 years. The formation is a deltaic clastic sequence with quartz and feldspar as main mineral composites. The injection target is a cross-bedded sand between 642 and 700m.

2. Modeling specifications

The salt precipitation due to CO_2 injection was modeled with the TOUGH2[3] code, using the fluid property module for CO_2 and brine systems, called ECO2N[4]. The problem was approached in several stages, from a very simple 1D radial model to a 2D model with several layers. The injection is modeled as non-isothermal, including molecular diffusion effects and capillary pressure functions.

For the absolute porosity-permeability relation and the impact of salt precipitation to the pore space, the "tubes-in-series" model was used. The simplest model that can capture the converging-diverging nature of natural pore channels consists of alternating segments of capillary tubes with larger and smaller radii, respectively. While in straight capillary tube models permeability remains finite as long pore body pore

throat as porosity is non-zero, in models of tubes with different radii in series, permeability is reduced to zero at a finite porosity. From the tubes in series model the following relationship can be derived [4]:

$$\frac{k}{k_0} = \theta^2 \frac{1-\Gamma+\Gamma/\omega^2}{1-\Gamma+\Gamma\left[\theta/(\theta+\omega-1)\right]^2}$$

, where k is the absolute permeability after the salt precipitation and k_0 the initial absolute permeability. θ is a function of solid saturation S_s and a fraction of original porosity Φ_r at which permeability is reduced to zero. Γ is the fractional length of the pore bodies, and ω a function of Φ_r and Γ.

The equation above has only two independent geometric parameters that need to be specified, Φ_r and Γ. As an example, Figure 1 shows the permeability reduction factor, plotted against $\Phi/\Phi_r \equiv(1-S_s)$, for parameters of $\Phi_r = \Gamma = 0.8$.

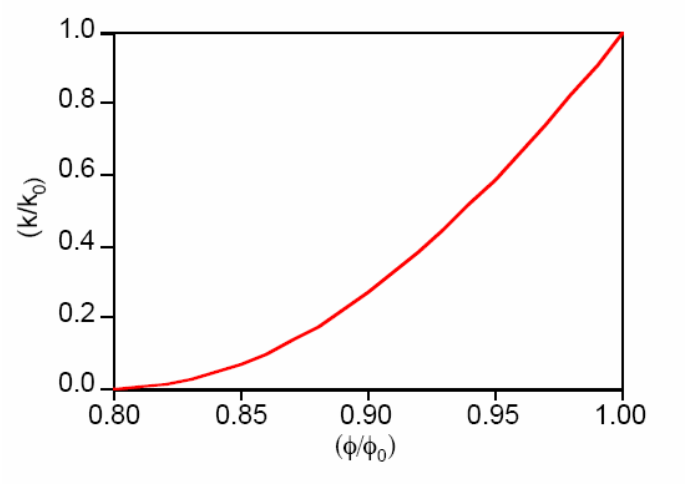

Figure 1. Porosity-permeability relationship for tubes-in-series model, after Verma and Pruess (1988).[4]

To capture the relative permeability behavior of the two miscible fluids CO_2 and water, an approximation to experimental data was used. Bennion and Bachu (2006) conducted core experiments on sandstones and carbonates with different absolute permeability, establishing several supercritical CO_2 and brine relative permeability relations.[5] From this work, the relative permeability relation of the Viking sandstone with an absolute air permeability of 5.78 mD was used to choose the appropriate relative permeability function. Since the experimental parameters are not the same as the reservoir properties, in regard to the absolute permeability, pressure and temperature conditions, we looked only for an approximate, but not absolute fit of the theoretical relative permeability model. The van Genuchten – Mulaem model seemed to be the best approximation, see Figure 2. The model can be described as follows[6]:

$$k_{rl} = \begin{cases} \sqrt{S^*}\left\{1-\left(1-[S^*]^{1/\lambda}\right)^{\lambda}\right\}^2 & \text{if } S_l < S_{ls} \\ 1 & \text{if } S_l \geq S_{ls} \end{cases}$$

, where k_{rl} is the relative brine permeability, S_{ls} the maximum brine saturation, S_l the brine saturation and λ defines the curvature of the relative permeability curves. CO_2 permeability can be chosen as one of the following forms, the second is the known Corey function[7].

$$k_{rg} = \begin{cases} 1-k_{rl} & \text{if } S_{gr}=0 \\ \left(1-\hat{S}\right)^2\left(1-\hat{S}^2\right) & \text{if } S_{gr}>0 \end{cases}$$

, where k_{rg} is the relative gas permeability, S_{gr} the residual gas saturation and $\hat{S} = (S_l - S_{lr})/(1 - S_{lr} - S_{gr})$.

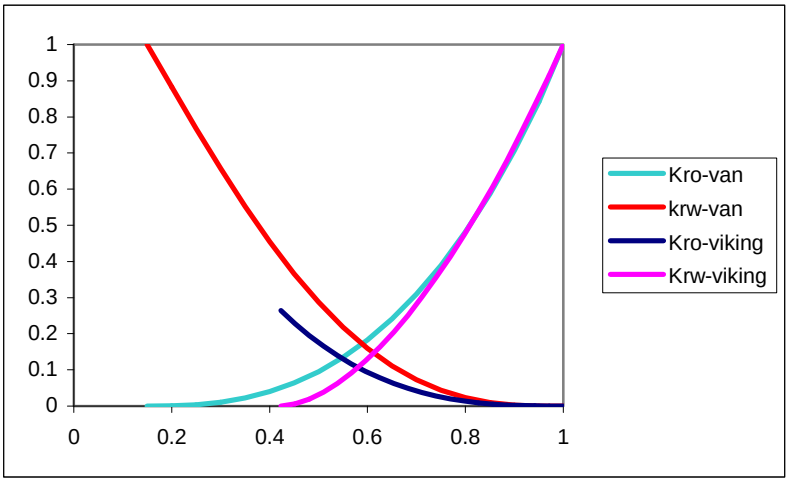

Figure 2. Relative permeability function comparison of experiment with theoretical model.

In above figure, "kro-van" presents relative permeability CO_2 and "krw-van" the relative permeability of brine of the van Genuchten – Mulaem model, using the following endpoints: $S_{lr} = 0.15$; $S_{ls} = 1$; $S_{gr} = 0.00001$; $\lambda = 0.96$. "kro-viking" and "krw-viking" are the experimental relative permeabilities of CO_2 and brine respectively.

III. PART ONE: 1D MODEL

Geometry. The 1D radial grid was generated with the TOUGH2 MESHmaker[5]. The grid is logarithmic and becomes coarser at further distance from the injection point (=well). The well has a radius of 0.2 m. From 0.2 m onwards the formation contains 100 grid cells in the first 100 m, increasing logarithmically. From a radius of 100 meters to 1000 m 200 grid cells are arranged logarithmically. From 1000 to 3000 m lie 100 grid blocks, and from 3000 to 10.000 are 100 grid cells. The outer most grid block is at 95 000 m distance from the well.

Reservoir and injection conditions. The temperature of 35°C and pressure of 65 bar imply sub critical conditions for CO_2 in the reservoir. Carbon dioxide is injected at 55°C and 73 bar at bottom hole conditions. For this particular example, we calculate with an injection rate of 1kg/s for two years. The injection formation is assigned as "sand" with bulk density of 2.6g/cc, average porosity of 12% and average permeability of 273 mD. The formation is filled with a 200 ppk NACl brine.

Boundary conditions. Fluid is injected into 18 m thick layer through an infinite dense gridblock (=well) to enable non-isothermal behavior. Other than that, the "well" grid block has the same properties as the injection formation. The outermost gridblock is at a distance of 95 000 m, providing no boundary conditions on the fluid flow.

1. Preliminary results

i) Dry CO_2 injection

In this model run dry supercritical CO_2 is injected into a sand formation containing a brine of 200 ppk salinity.

At the onset of injection gaseous CO_2 dissolves into the brine. At a certain gas saturation the effect reverses and water is dissolved into CO_2 (see Figure 3, gas saturation is plotted by the y-axis on the left, and the dissolved CO2 on the right y-axis).

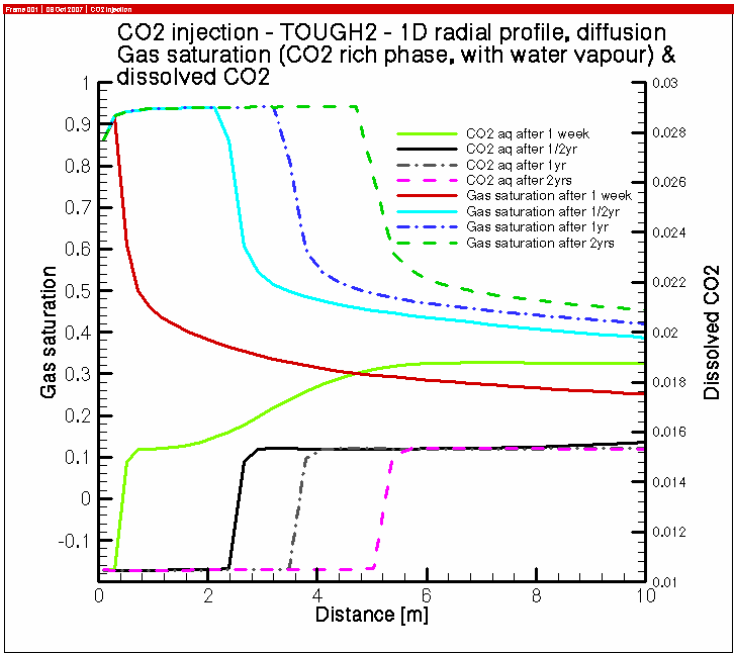

Figure 3. Gas saturation (CO_2 rich phase) and the dissolution of CO_2 into brine close to injection point.

Note that the carbon dioxide starts taking up formation water only close to the borehole. This is illustrated in Figure 3 by the gas saturation lines after 1 week, half a year, one year and two years of injection. The liquid phase becomes heavier the more water evaporates (see Figure 5). The liquid phase consists of water, dissolved salt in form of halite (NaCl) and carbon dioxide. In Figure 5 the density of the liquid phase is plotted on the y-axis versus the distance from the borehole on the x-axis.

Figure 4 shows that the concentration of dissolved NaCl increases sharply before the onset of solid precipitation. The solids are the salt precipitating from the brine (see Figure 4). The concentration of the salt in solution, plotted at the left y-axis, and the salt solids, on the right y-axis, mirror the density behavior.

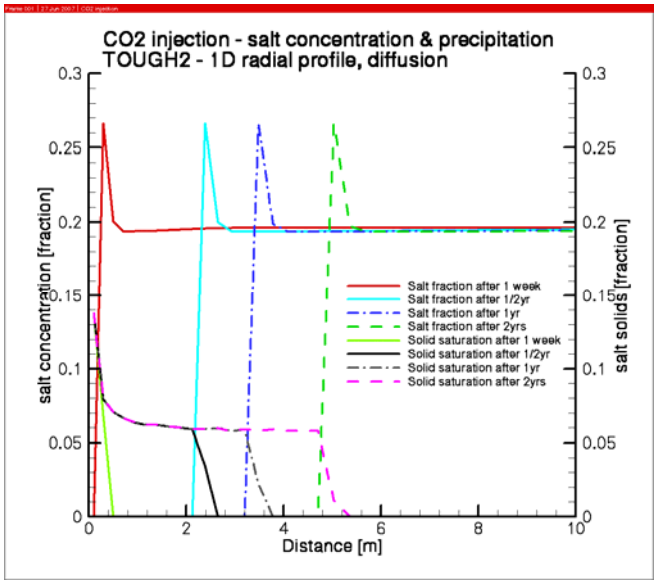

Figure 4. Precipitation of halite close to the borehole due supercritical drying of CO_2.

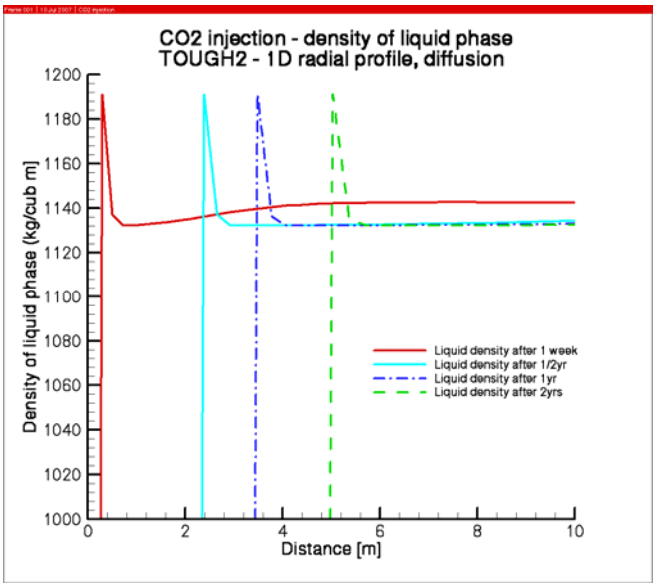

Figure 5. Variation of the densities of the liquid phase in the proximity of the borehole.

The halite precipitation leads to a pore geometry change. The absolute permeability is reduced by 50% (see Figure 6). The permeability reduction is plotted as factor of the absolute permeability on the y-axis. The injection capacity can be limited by the permeability reduction up to 5 m into the formation (see Figure 6). Formation pressure increases during the CO_2 injection. Figure 7 shows that the pressure propagates further into the formation compared to the actual fluid interactions. The pressure at the injection point is close to injection pressure of 73 bar, plotted on the y-axis in Pascal versus distance from the injection point on the x-axis. After two years of CO_2 injection the pressure has risen well above of initial formation pressure of 65 bar to 70.4 bar at 400 m from the injection point.

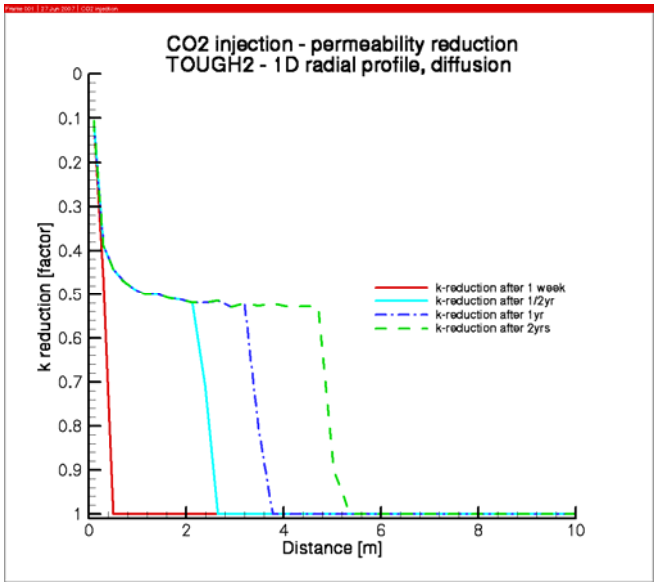

Figure 6. Permeability reduction due to salt precipitation.

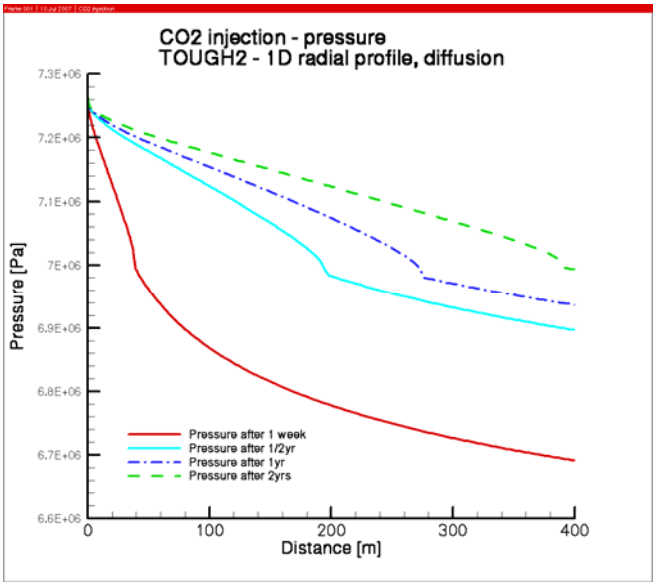

Figure 7. Injection pressure propagation in the formation at 1 week, 1/2 yr, 1 yr and 2 yrs.

To evaluate how fast this effect takes place, the phase evolution in a gridblock over time was monitored (see Figure 8). The particular gridblock is at 2.7 m distance from the injection point. At 2.7 m distance the salt concentration in the brine increases with continued CO_2 injection, until it reaches equilibrium after 8.7 hours. At this point salt starts precipitating (see onset of saturation curve in Figure 8) and keeps on accumulating until the formation is completely dried up (salt concentration drops to zero in Figure 8). After 2.6 days no more salt is precipitated and the gas saturation is stable. During and after the "evaporation" pressure varies slightly and builds up over time. This can be attributed to the increased fluid volume and mounting decrease of porespace.

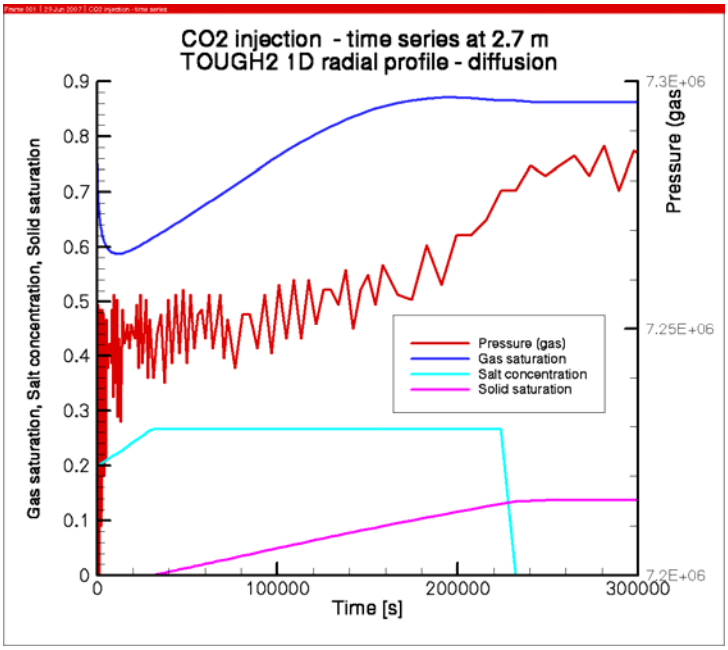

Figure 8. Time series of aqueous concentrations, gas saturation and gas pressure [Pa] at 2.7 m distance from the borehole (grid block 12) until 3.4 days.

ii) After CO2 injection

This model projects the events after CO_2 injection has stopped.

Formation water starts to re-invade the dried out zone close to the borehole. The re-invasion occurs slowly as Figure 9 demonstrates (salt concentration on the y-axis versus distance from injection point at several time snapshots: after 1 year, 3, 10, 100, 300 and 10.000 years of CO_2 injection stop). The 1D model has no inclination. Therefore neither buoyancy and nor gravity forces have an influence, only capillary and formation pressure drive the re-invasion. Fluid is allowed to flow across the "well" gridblock though. After 300 years the salt in solution stabilizes at higher than initial concentrations close to the borehole (see blue and green dashed curve in Figure 9). 26.3% appears to be the salt solubility limit of the system.

The gas saturation close to the borehole stays almost 100% for a century (see Figure 10). After a hundred years the gas saturation has decreased significantly (see Figure 10). However, the gas keeps on dissolving in minute quantities into the liquid phase. The gas progresses slowly further out into the formation, until 550 m, where it reaches equilibrium after 10.000 years (see dashed curve in Figure 10).

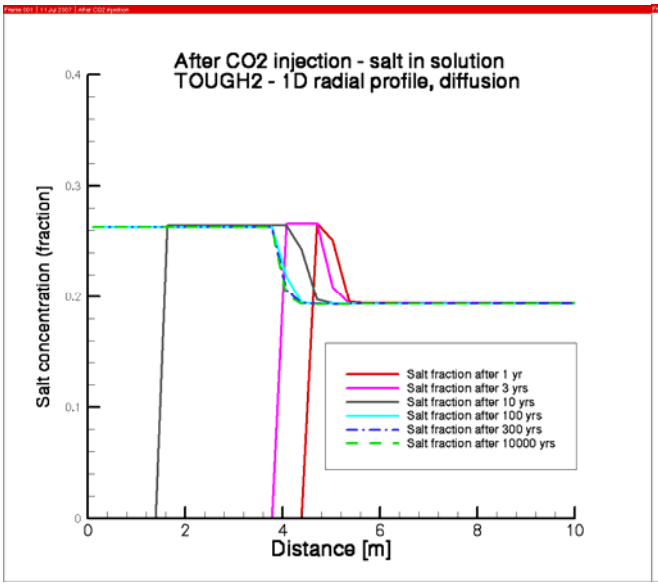

Figure 9. Formation water re-invades dry zone, the salt in solution is stable after 300 yrs.

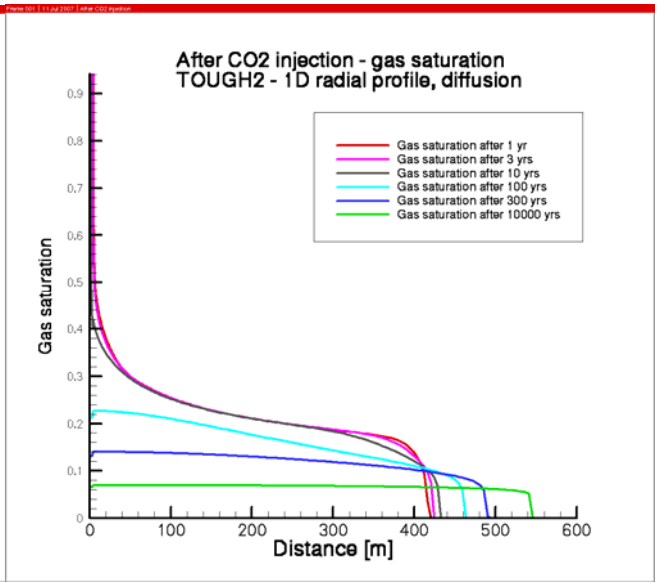

Figure 10. Gas saturation close to the borehole remains high for decades and will decrease after a century.

The re-invading formation water dissolves the precipitated salt (see Figure 11) up to the solubility limit of 26.3% (see Figure 9). The solid fraction remains unchanged close to the borehole even after 10.000 years (see dashed curve in Figure 11). This is reflected in the absolute permeability reduction shown in Figure 12. The 50% absolute permeability reduction front retreats from 5.5 m to 3.6 m distance from the well. The absolute permeability remains almost 100% impaired near the wellbore (see Figure 12).

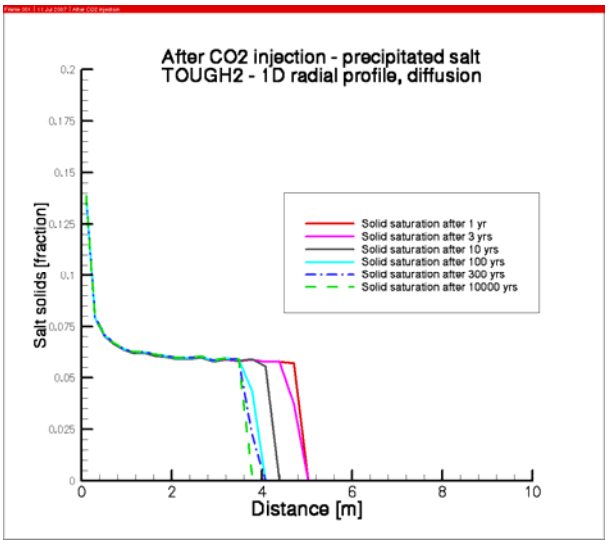

Figure 11. Salt precipitation changes slowly after injection stop due to re-invading formation water.

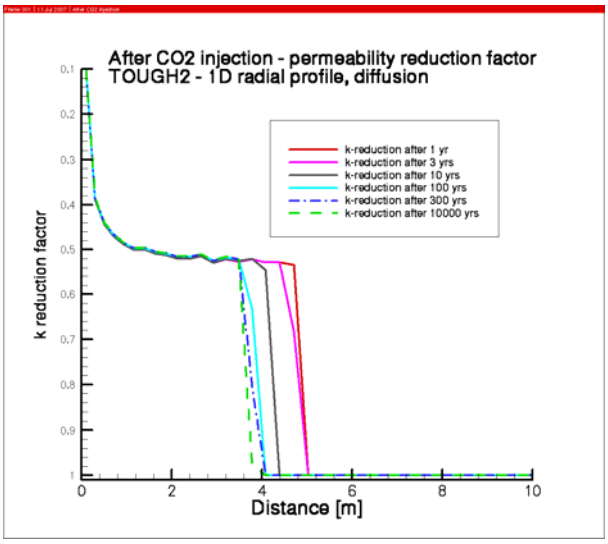

Figure 12. Permeability is gradually restored due to re-invading formation water.

Pressure returns close to initial conditions of 65 bar after 10 years, see also pressure curve in Figure 13. Although only minor fluctuations occur does formation pressure remain unstable beyond 10.000 years (see Figure 13). The pressure propagation coincides with the gas saturation in Figure 10. After 10.000 years pressure has increased up to 550 m distance from the borehole.

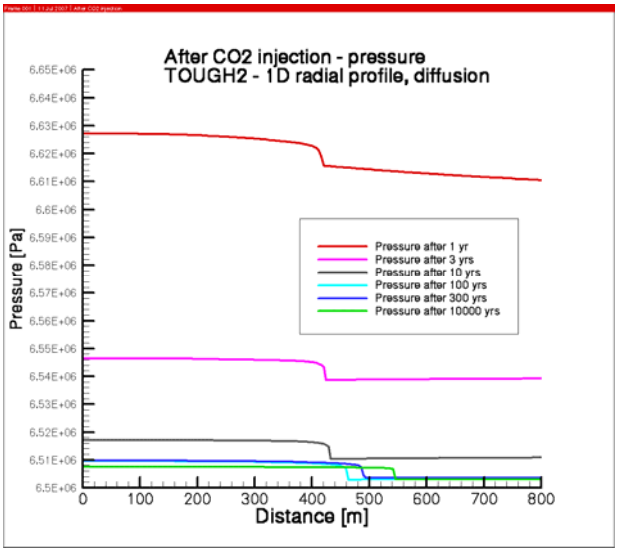

Figure 13. Pressure returns close to initial conditions after 10 yrs.

The pressure fluctuation can also be observed in the time series plot in the gridblock at 2.7 m distance from the borehole (see Figure 14). Formation water re-invades that particular reservoir section after 7.3 years, indicated by the salt concentration curve coming up from zero to 26.3% in Figure 14. 6% of the available porespace remain saturated with solids (=precipitated salt), see dashed line in Figure 14. Gas phase CO_2 decreases from 100% to 21%. Although the gas amount decreases significantly, only a little CO_2 dissolves in water. Most of the gas migrates further out into the formation (see Figure 10).

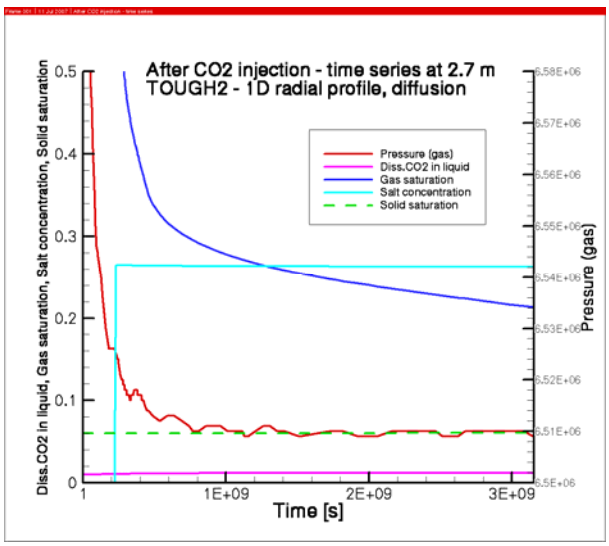

Figure 14. Time series of aqueous NaCl, salt solids, gas saturation and pressure at 2.7 m distance from the borehole (gridblock 12) until 100 years after CO_2 injection stop.

IV. SUMMARY AND OUTLOOK:

Halite precipitation could have a severe impact on the injectivity of CO_2 in an average permeable reservoir. Due to the mutual solubility of water and CO_2, the precipitated salt from the formation water can potentially block almost 100% of the available pore throats at the injection point and prevent any further injection. There are simple reservoir engineering techniques available that could remediate halite precipitation. One solution could be pre-flushing the formation close to the borehole with freshwater and inject CO_2 after the fresh water flood. The high salt concentration front would be at further distance from the injection point. Halite precipitation would still occur, but less spatially concentrated. Thus, the permeability impaired at the injection point would be less severe.

Furthermore, to get a better idea of how the salt precipitation takes place in a 3 dimensional pore space, the effect needs to be studied in 2 D and 3D models as well as laboratory experiments.

The next step of this work is to study

1. Model the CO_2 injection after a fresh water preflush
2. Model the halite precipitation effect in 2D and 3D models
3. Parallel to above efforts, conduct lab experiments on cores.

V. REFERENCES:

[1] Spycher, N. and Pruess K., "CO2-H2O Mixtures in the Geological Sequestration of CO2. II. Partitioning in Chloride Brines at 12–100 °C and up to 600 bar", *Geochim. Cosmochim. Acta*, Vol. 69, No. 13, pp. 3309–3320, 2005.

[2] Kleinitz W., Koehler M., Dietzsch G., "The precipitation of salt in gas producing wells", SPE 68953, 2001.

[3] Pruess K., "The TOUGH codes - A Family of Simulation Tools for Multiphase Flow and Transport Processes in Permeable Media", Vadose Zone Journal, Vol. 3, pg.738–746, Soil Science Society of America, 2004.

[4] K. Pruess, "ECO2N: A TOUGH2 Fluid Property Module for Mixtures of Water, NaCl, and CO2", Lawrence Berkeley National Laboratory, Paper LBNL-57952, August 2005.

[5] Bennion D.B., Bachu S., „Supercritical CO2 and H2S – brine drainage and imbibition relative permeability relationship for intergranualr sandstone and carbonate formations", SPE 999326, 2006.

[6] Pruess K., Oldenburg C., Moridis G., "TOUGH2 USER'S GUIDE, VERSION 2.0", Lawrence Berkeley National Laboratory, Paper LBNL-43134, November 1999.

[7] Corey, A.T., "The Interrelation Between Gas and Oil Relative Permeabilities", Producers Monthly, 38-41, November 1954.